

Application of the critical gradient concept to the nucleation of the first-product phase in Co/Al thin films

M. O. Pasichnyy,¹ G. Schmitz,² A. M. Gusak,¹ and V. Vovk²

¹*Department of Theoretical Physics, Cherkasy National University, Shevchenko Str. 81, 18031 Cherkasy, Ukraine*

²*Institute für Material Physics, Westfälische Wilhelms-Universität, Wilhelm-Klemm-Str. 10, 48149 Münster, Germany*

(Received 10 March 2005; revised manuscript received 23 May 2005; published 18 July 2005; publisher error corrected 21 July 2005)

Recent high resolution analysis by atom probe tomography demonstrated that the first reaction product in Al/Co reaction couples, the phase Al_9Co_2 , is only nucleated after interdiffusion of the pure elements on a depth of about 4 nm. In this article numerical calculations are presented to investigate, whether critical gradient concepts based on thermodynamic considerations are suitable to understand the observed retardation of nucleation. Different microscopic nucleation mechanisms are considered. It is found that the formation of the nucleus by a polymorphic transformation inside the diffusion zone provides a quantitative agreement with experimental data.

DOI: [10.1103/PhysRevB.72.014118](https://doi.org/10.1103/PhysRevB.72.014118)

PACS number(s): 64.70.Nd, 66.30.Pa, 68.55.Ac

I. INTRODUCTION

The nucleation of product phases during reactive interdiffusion has recently attracted considerable interest, since with downscaling of structures into the nanometer range the earliest stages of phase formation become important. Compared to nucleation in decomposition processes, for which a rather clear theoretical framework has already been developed, in the case of reactive diffusion even fundamental ideas are still a matter of controversy. The main difficulty arises from the extreme gradient in composition that exists initially at the interface. As a consequence, besides nucleation of a distinct product phase, intermixing by volume diffusion always provides a competing reaction path. Based on only thermodynamic considerations, Desré *et al.*¹ as well as Gusak² introduced the concept of a critical composition gradient, above which nucleation is forbidden. However in the details of the nucleation mechanism both authors apply different microscopic schemes, and furthermore, these were modified and refined later.³ Actually one may distinguish between the polymorphic, the transversal, and the complete mixing scheme. Only the former two predict an initial suppression of the nucleation event by an increase of the nucleation barrier, while for the latter scheme the driving force for nucleation is even increased by the chemical gradient. On the ground of purely thermodynamic considerations, one has to argue that nature will choose the path of lowest nucleation barrier and so, only the total mixing mode would realistically describe the nucleation event. However, as soon as kinetic aspects are considered, the situation gets quite complicated, since the mobility may be too low to achieve the intermixed state inside the nucleus. A detailed theoretical description of this complex situation is still lacking.

Sound experimental checks of the different nucleation modes are rare. This is mainly due to the fact that predicted critical gradients are so high that atomic transport must be investigated on length scales down to a few nanometers only. Thus, local analysis of outstanding spatial resolution is required. In extreme cases, the critical diffusion depth gets even smaller than the lattice parameter of the expected prod-

uct phase. Then, the concept of nucleation suppression by a loss of thermodynamic driving force is no longer feasible.

A method of spatially resolved chemical analysis is provided by atom probe tomography (TAP), which is ideally suited for the investigation of metallic thin reaction couples.^{4,5} Recently, the reaction of Co/Al thin films has been studied with this technique.⁶ According to previous studies of this binary system,^{7,8} the first phase to nucleate and to grow in the temperature interval from 200 to 400 °C is Co_2Al_9 . The process of nucleation at the initial interface was traced by the TAP. Prior to the formation of the expected intermetallic, thin-film couples demonstrated the formation and broadening of a solid solution (intermixing) layer. Obviously, the appearance of the product phase is controlled by the width of this zone, since particles of the product phase Co_2Al_9 are never observed before the diffusion zone reached about 3–4 nm in thickness. To our knowledge, this is a unique case, in which for a metallic system the retardation of the first phase is clearly demonstrated. Usually, the first phase (stable or metastable) forms immediately and changes the conditions for the formation and growth of the second phase, so that the latter may be suppressed owing to kinetic⁹ or thermodynamic reasons.¹⁰

According to d'Heurle,¹¹ the fastest growing phase is usually also nucleated first, since this phase is distinguished by a high atomic mobility. In our case Co_2Al_9 is clearly the first and the fastest growing phase. Therefore it is difficult to explain the retardation of just this phase by kinetic arguments. As a consequence, the present paper considers the possibilities of thermodynamic suppression. The total driving force for the formation of Co_2Al_9 from the pure elements is rather high. Furthermore the specific energy of the interfacial energy between nucleus and parent phase is quite moderate so that the theoretical limit of the nucleation thickness is estimated to only $d=2\sigma/g_0=0.2$ nm. Thus, in a naive picture, one should not observe any barrier to nucleation at all. Yet, according to the concept of critical gradient the total driving force cannot be applied in full to the nucleation process. By a comparison of the behavior predicted by the suggested nucleation modes with the experimental one, we will

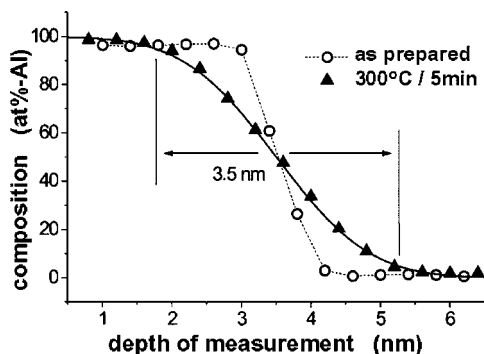


FIG. 1. Composition profiles of Al determined normal to the Al/Co interface in the as-prepared state and after 5 min annealing at 300 °C according to the data in Ref. 6. The solid line represents the error function solution of thick film interdiffusion.

figure out, which mode if any will provide a realistic description of the nucleation event. Since only the polymorphic and transversal mode predict a thermodynamic suppression by sharp concentration gradients, we present a numeric analysis of the nucleation of Co_2Al_9 via transversal and polymorphic modes.

II. BASIC MODEL

According to the atom probe analysis, the concentration profile of the couple Co/Al, prior to nucleation of the first product phase, is continuous and can be well approximated by the error-function-shaped solution of Fick's Laws (see Fig. 1), thus:

$$c(x, L) = \frac{c_r + c_l}{2} + \frac{c_r - c_l}{2} \operatorname{erf}\left(\frac{x}{L}\right), \quad (1)$$

where c_r and c_l denote the atomic fractions of Co in the "right" and "left" terminating layers. In order to avoid numerical problems with chemical potentials of very dilute solutions the terminating compositions are chosen to be 0.01 and 0.99 instead of 0 and 1. L denotes the characteristic length of the diffusion zone. For the comparison with the experimental data, we define the width K of the diffusion zone in agreement to Ref. 6 as the distance $x_2 - x_1$ between the positions with the concentrations $c(x_1, L) = 0.05$, $c(x_2, L) = 0.95$. Between L and K the numerical ratio of $K = 2.46L$ holds.

We consider the potential nucleation in the inhomogeneous intermixed zone. The nucleus of the intermetallic phase is supposed to be a rectangular parallelepiped with sizes $2R \times 2h \times 2h$ (Fig. 2).

The thermodynamics of the diffusion zone before nucleation (inhomogeneous parent phase) is treated as an ideal solution with a Gibbs potential per one atom of parent phase according to

$$g_o(c) = kT[c \ln(c) + (1 - c)\ln(1 - c)], \quad (2)$$

where k and T are Boltzmann constant and absolute temperature, respectively. In a strict sense, one should model the solution at least as a regular one, but the formation enthalpy

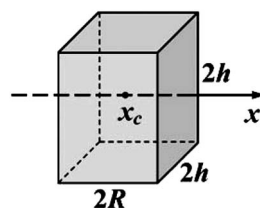


FIG. 2. New phase nucleus with the shape of a rectangular parallelepiped sized $2R \times 2h \times 2h$ and its geometrical center at the point x_c . The concentration gradient in the parent phase is directed along the x -axis.

of the regular solution is much less than the driving force to form the intermetallic compound. Thus, neglecting the mixing enthalpy in the parent phase will not lead to any substantial error. Due to the pronounced variation in composition within the diffusion field, the Gibbs energy per atom as well as the local driving force to nucleation is a function of coordinates. The thermodynamic modelling of the intermetallic product phase is done in quadratic approximation, thus

$$g_n(c) = g_1 + \frac{\alpha}{2}(c - c_n)^2, \quad (3)$$

where $c_n = 2/11$ denotes the ideal stoichiometric composition of the intermetallic, g_1 the Gibbs free energy per atom for stoichiometric composition, and the parameter α describes the curvature of the thermodynamic potential. The formation of the nucleus within the concentration field leads to a change in Gibbs energy that can be written in general as

$$\Delta G(\varphi, R, x_c) = 4n\varphi^2 R^2 \int_{x_c - R}^{x_c + R} \Delta g(c(x)) dx + 8\sigma\varphi R^2(2 + \varphi), \quad (4)$$

where φ , n , σ , and $\Delta g(c)$ denotes a shape factor $\varphi := h/R$, the number of atoms per unit volume, energy of the interface (per unit area) between nucleus and inhomogeneous matrix, and the thermodynamic driving force to form the nucleus (change of bulk Gibbs energy per atom of nucleus), respectively. The different nucleation modes are distinguished by different driving forces $\Delta g(c)$ and thus different nucleation barriers. However, the choice among these modes is not only controlled by the height of the nucleation barrier but by kinetic factors as well.^{12,13}

In view of the Cahn-Hilliard and modern phase field approaches, one may replace the last term on the right-hand side of Eq. (4) by gradient energy terms in quadratic dependence on the gradients of composition and of some order parameter describing the structural transformation. But already Desré pointed out that in the transversal mode the influence of the concentration gradient energy on the nucleation barrier is negligible.¹⁴ Yet, in a polymorphic nucleation the composition gradient does not change at all. Thus, there is no first order impact by the respective gradient energy, too. The interface between the intermetallic and the parent lattice is reasonably assumed to be incoherent from the very beginning. Beside the incompatible lattice structures, this assumption is confirmed by the growth kinetics of the nuclei, which

TABLE I. Total driving force per atom for the formation of intermetallic phases in the Co/Al system. Data at 298 K and 773 K were taken from Ref. 7. The important value for 573 K was obtained by linear interpolation.

T, K	$\Delta G_f^{Al_9Co_2}, \frac{J}{atom}$	$\Delta G_f^{Al_{13}Co_4}, \frac{J}{atom}$
298	-5.5×10^{-20}	-6.5×10^{-20}
573	-5.0×10^{-20}	-6.0×10^{-20}
773	-4.7×10^{-20}	-5.6×10^{-20}

was observed in the TAP analysis and quantitatively discussed.⁶ As a consequence, the variation of lattice structure is restricted to the narrow interphase boundary, so that a sharp interface characterized by a specific energy is a quite reasonable approximation. The change in molar volume by the lattice transformation is rather low ($\Delta V/V \approx 0.03$).⁷ Elastic contributions to the nucleation energy are therefore negligible.

We treat the change in Gibbs energy as a function of the shape parameter φ of the nucleus volume v , $v = 8\varphi^2 R^3$, and of the concentration c_x at the nucleus center x_c . The nucleation barrier ΔG^* is defined by the saddle point of the surface $\Delta G(\varphi, v, c_x)$, satisfying the set of the following conditions:

$$\begin{aligned} \frac{\partial \Delta G}{\partial \varphi} = 0, \quad \frac{\partial^2 \Delta G}{\partial \varphi^2} > 0, \quad \frac{\partial \Delta G}{\partial v} = 0, \quad \frac{\partial^2 \Delta G}{\partial v^2} < 0, \\ \frac{\partial \Delta G}{\partial c_x} = 0, \quad \frac{\partial^2 \Delta G}{\partial c_x^2} > 0. \end{aligned} \quad (5)$$

To determine the nucleation barrier ΔG^* numerically, we proceed in the following way. The possibility of nucleation at each position of parent solution is considered. At this position of the nucleus center we increase (step by step) the nucleus volume, optimizing the shape parameter at each step. Finally the position corresponding to the minimum nucleation barrier is chosen. A more detailed description of the structure of the optimization algorithm is presented in the Appendix.

The thermodynamic parameters required for the calculation were taken from data published in Ref. 7. Since the nucleation of Al_9Co_2 was observed experimentally at 573 K, the Gibbs enthalpy of phase formation for this temperature was determined by linear interpolation of literature data, see Table I. Also a quantitative value for the specific energy of the incoherent phase boundary was taken from Ref. 7. The final parameters used for the numerical evaluation are stated in Table II.

III. NUMERICAL RESULTS

With the above explained algorithm the composition and size dependence of the Gibbs nucleation energy were calculated for the two nucleation modes under consideration and for various interdiffusion widths. As already mentioned, both modes are distinguished by different driving forces and may

TABLE II. Numerical parameters for the Co_2Al_9 phase at 573 K, used for the calculation.

$n, \frac{atom}{m^3}$	$g_1, \frac{J}{atom}$	T, K	$\sigma, \frac{J}{m^2}$
6.6×10^{28}	-5.0×10^{-20}	573	0.35

only take place in restricted compositional ranges. A schematic overview indicating the driving forces and composition ranges is shown in Fig. 3. In the following numerical results are presented.

A. Transversal mode

The transversal mode was introduced by Desré.¹ It means that the nucleus of the new phase is constructed from thin transversal slices (perpendicular to gradient direction), each of which is formed as a result of redistribution of components between new and parent phases only inside this slice. The composition of the parent phase varies from slice to slice due to the compositional gradient and thus, the local driving force varies as well. Therefore, the composition of the new phase and the driving force is determined individually for each slice from the composition of the respective parent phase according to the rule of parallel tangents.

For the Gibbs energy $g_n(c)$ of the nucleus phase the expression according to Eq. (3) is used. Since the Al_9Co_2 phase is a line compound, the curvature parameter α must be rather large, so that in view of the tangent rule $\alpha \rightarrow \infty$ may be assumed to good approximation. Thus, we have for the driving force per atom of the nucleus

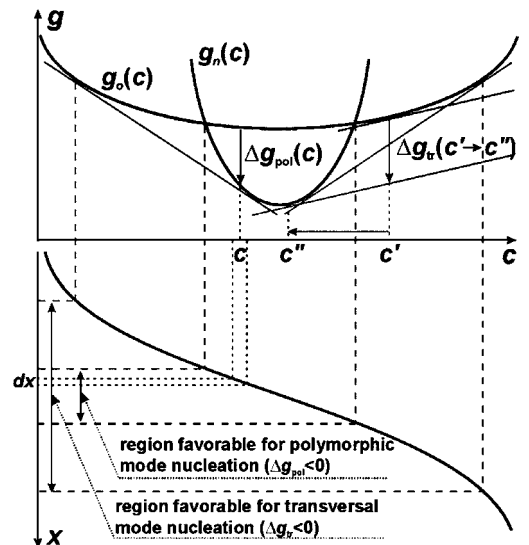


FIG. 3. Schematic figure on the thermodynamic basis of the nucleation modes. Here $\Delta g_{pol}(c)$ means the driving force of polymorphic transformation without change of local composition $c(x)$ in a slice $dx = dc / (\partial c / \partial x)$. $\Delta g_{tr}(c' \rightarrow c'')$ represents the local driving force for the transversal mode, for which a slice of the new phase with composition c'' is formed by transversal redistribution from a slice of the parent phase with composition c' .

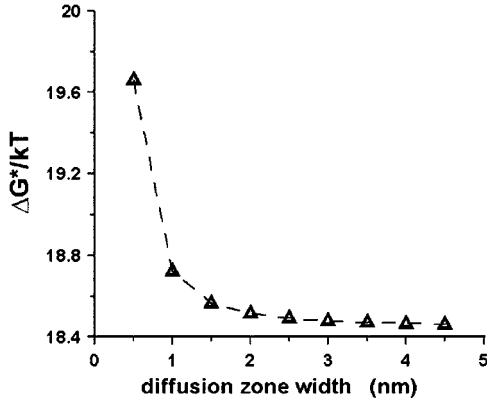


FIG. 4. Nucleation barrier of Co_2Al_9 nucleus formation at the Al/Co interface calculated by the transversal mode without shape optimization for different diffusion zone widths.

$$\Delta g(c) = g_1 - g_o(c) + (c - c_n) \left. \frac{\partial g_o}{\partial c} \right|_c. \quad (6)$$

Numeric analysis of Eq. (4) with $\Delta g(c)$ in the form of Eq. (6) was made for different widths of the diffusion zone down to $K=0.5$ nm. We considered two different cases: (i) without shape optimization (nucleus being a cube $2R \times 2R \times 2R$; the inner loop for the optimization of the shape parameter is excluded from the algorithm and the shape parameter is fixed at $\varphi=1$) and (ii) with shape optimization, i.e. for each nucleus volume φ is determined to minimize ΔG .

The calculated results demonstrate in both cases that even at a very narrow interdiffusion width the nucleation barrier is rather low, about $20 kT$ (Fig. 4) and the critical size $2R_{cr}$ of the nucleus amounts to 0.45 nm. A significant influence of the compositional gradient is only predicted for a diffusion zone of 1 nm width or less.

This result obviously contradicts the experimental observation that the Co_2Al_9 phase appears only for a diffusion zone larger than 3 nm. Moreover, the mentioned critical size is less than the size of one structural unit of the Al_2Co_9 phase. Its monoclinic unit cell actually includes 22 atoms and its lattice parameters range from 0.6 to 0.8 nm. There-

fore, we can conclude that the transversal mode is not relevant for the nucleation of Al_9Co_2 in Co/Al couples.

B. Polymorphic mode

The polymorphic mode of nucleation is characterized by the conservation of the concentration profile, which is a reasonable assumption if the system has no time to redistribute atoms inside and outside the nucleus in the process of lattice transformation. For the polymorphic mode we also considered the two cases: (i) without shape optimization ($\varphi=1$); and (ii) with shape optimization.

In the case of polymorphic mode, the finite curvature of the Gibbs energy can no longer be neglected. Thus, α in Eq. (3) equals $\partial^2 g_n / \partial c^2$, which is a finite constant in the case of parabolic approximation. Regarding that the local concentrations do not change during nucleation, the driving force is represented by

$$\Delta g(c) = g_n(c) - g_o(c). \quad (7)$$

For each value of the curvature parameter α one finds a critical zone width K^* , at which nucleation by polymorphic mode becomes possible. We define this critical width by the postulation that the nucleation barrier becomes higher than $60 kT$ for all $K < K^*(\alpha)$ (nucleation suppressed). Unfortunately, no direct measurements of the curvature of the Gibbs potential of the Al_9Co_2 phase are known. Therefore, in order to compare with the experiment, we will first determine by our calculations the value of α so that the predicted critical width agrees to the experimental finding ($K^*=3.5$ nm) and will later discuss the relevance of this numerical value.

1. Polymorphic mode without shape optimization

Numeric analysis at $\alpha=8 \times 10^{-18}$ J/atom leads to the following results: At zone width of $K=3$ nm the surface $\Delta G(v, c_x)$ has no saddle-point at all [Fig. 5(a)]. For any c_x the dependence $\Delta G(v)$ is monotonically increasing. In other words, at this zone width the nucleation of Co_2Al_9 is still thermodynamically suppressed.

Already a slight increment of the zone width to $K=3.5$ nm leads to formation of a local minimum at the sur-

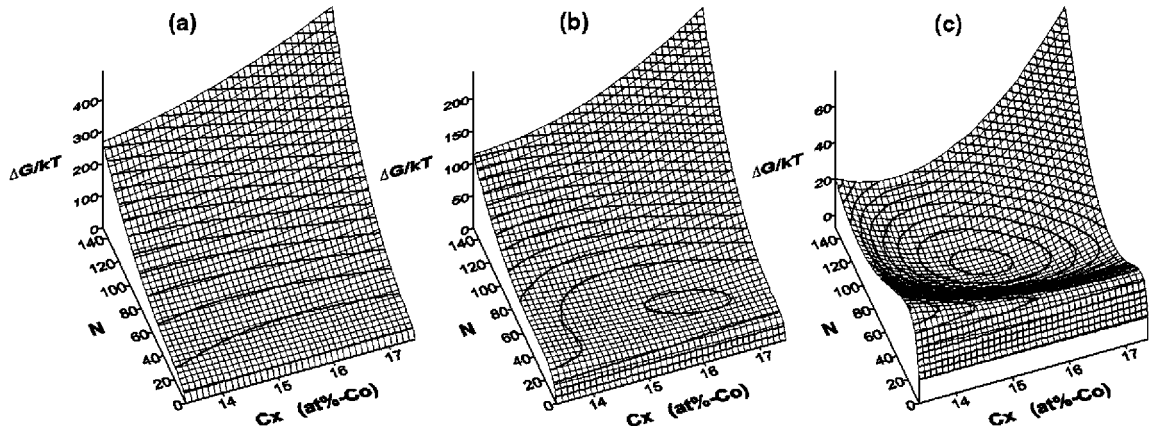


FIG. 5. Surface $\Delta G(N, c_x)$ for the polymorphic mode without shape optimization ($\varphi=1$) at $\alpha=8 \times 10^{-18}$ J/atom for diffusion zone widths: (a) $K=3.0$ nm; (b) $K=3.5$ nm; (c) $K=4.0$ nm. Here N is the number of atoms in the new phase nucleus ($N=nv$) and c_x is the atomic fraction of species B at the center of the nucleus.

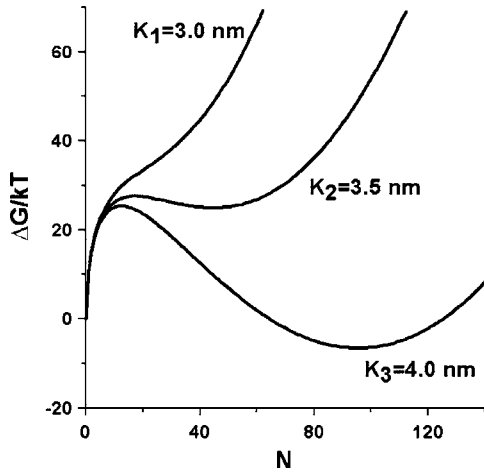


FIG. 6. Section through the $\Delta G(N, c_x)$ surfaces for the polymorphic mode without shape optimization at a composition $c_x = 15$ at %. ($\alpha = 8 \times 10^{-18}$ J/atom, calculation for different diffusion zone widths: $K_1 = 3.0$ nm; $K_2 = 3.5$ nm; $K_3 = 4.0$ nm.)

face $\Delta G(v, c_x)$ [Fig. 5(b)], which is still of positive magnitude corresponding to a metastable state (Fig. 6). A saddle point is found which allows determining a nucleation barrier. At $K = 4.0$ nm the minimum crosses the zero level and becomes negative [Fig. 5(c)], meaning that the intermediate phase becomes stable. The corresponding nucleation barrier ΔG^* appears to be only $25 kT$ (Fig. 6). The state of the local minimum corresponds to a nucleus containing about 100 atoms (linear size about 1.2 nm). Interestingly, composition at its geometrical center amounts to 15 at % in significant deviation of the intermetallic's stoichiometry (18.2 at %, which is due to the asymmetry of the error-function-shaped diffusion profile with respect to the nucleus center.

The mentioned nucleation barrier is rather low, which means that immediately after the diffusion zone in the parent phase reaches a width of 3.5 nm, the nucleation starts, and the intermediate phase appears.

2. Polymorphic mode with shape optimization

If the system has the kinetic opportunity of shape optimization, the resulting nucleation barrier decreases, as expected. Contrary to the situation in (i), the surface $\Delta G(v, c_x)$ does not reveal a minimum. After passing the saddle point it is always favorable to increase the volume by transversal growth, but keeping the longitudinal dimension along the direction of the gradient limited. A critical diffusion zone width, close to the experimental value, is obtained at $\alpha = 4 \times 10^{-17}$ J/atom. That means, for this parameter α and the diffusion zone width $K = 3.5$ nm, the nucleation barrier appeared to be $50 kT$ (Fig. 7), which corresponds to the upper limit for a barrier that allows nucleation at a reasonable time. The calculated longitudinal size of the critical nucleus amounts to 0.4 nm. Since this value is still smaller than the dimension of a single unit cell of the intermetallic compound, it is indicated that a full shape optimization during nucleation is a somewhat unrealistic assumption.

IV. DISCUSSION

The presented model calculations indicate indeed that the concentration gradient concept based on a polymorphic

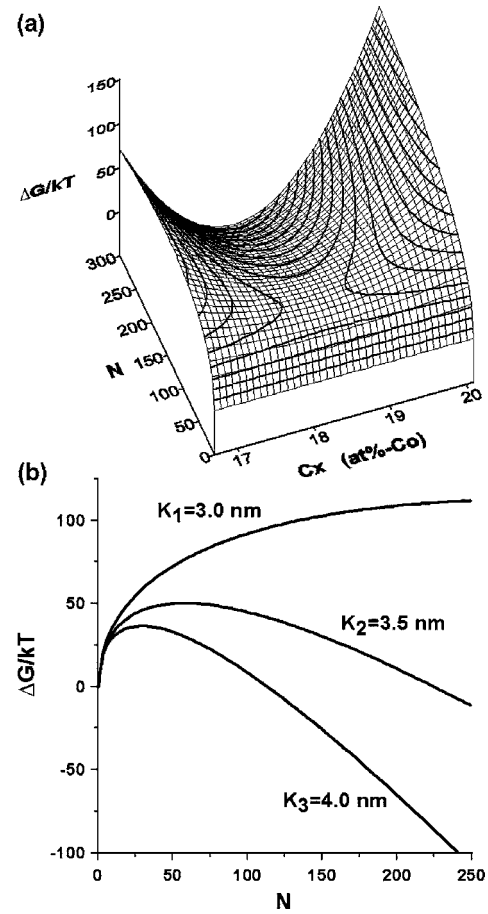


FIG. 7. Polymorphic mode with shape optimization at $\alpha = 4 \times 10^{-17}$ J/atom: (a) surface $\Delta G(N, c_x)$ for diffusion zone width 3.5 nm; (b) section $\Delta G(N, c_x)$ at $c_x = 18$ at % for diffusion zone widths $K_1 = 3.0$ nm, $K_2 = 3.5$ nm, and $K_3 = 4.0$ nm. (N is the number of atoms in the new phase nucleus, c_x is the atomic fraction of species B at the center of the nucleus.)

nucleation mode may quantitatively describe the observed retardation of the first product in the case of Al/Co. However, this statement is bound to the curvature of the Gibbs potential of the intermetallic phase. It is important to check, whether the figures used for the calculation, α about 10^{-17} J/atom, are reasonable. Since no direct measurements or explicit calculations of the respective Gibbs energy function are known, we need to estimate this value from known data of the phase stabilities. The approximate value of $\partial^2 g_n / \partial c^2$ can be found by

$$\frac{\partial^2 g_n}{\partial c^2} \approx \frac{\left. \frac{\partial g_n}{\partial c} \right|_{c_R} - \left. \frac{\partial g_n}{\partial c} \right|_{c_L}}{\Delta c}, \quad (8)$$

where $\Delta c = c_R - c_L$, c_R and c_L the compositions of the considered intermetallic compound in equilibrium to the “right-hand” neighbor phase $\text{Al}_{13}\text{Co}_4$, and to the “left-hand” terminating Al, respectively. A sketch of the thermodynamic situation is shown in Fig. 8. Furthermore, the values of the derivations with respect to composition, $m_2 = \partial g_n / \partial c|_{c_R}$ and

APPENDIX: ALGORITHM STRUCTURE FOR THE CALCULATION OF THE NUCLEATION BARRIER

Cycle for x_c resulting in $\Delta G^* = \min_{x_c} \Delta G(x_c)$:
 Cycle for v resulting in $\Delta G(x_c) = \max_v \Delta G(v, x_c)$ at the fixed x_c :
 Cycle for φ resulting in
 $\Delta G(v, x_c) = \min_{\varphi} \Delta G(\varphi, v, x_c)$ at the fixed v and x_c :
 Determine value of R for given v and φ :
 $R = \sqrt[3]{v/8\varphi^2}$;

Cycle for x from $x_c - R$ to $x_c + R$ (integration) resulting in $\Delta G(\varphi, v, x_c)$:
 $\Delta G^{\text{bulk}} := 4n\varphi^2 R^2 \sum_i \Delta g(c(x_i)) dx$;
 End of cycle for x .
 $\Delta G(\varphi, v, x_c) := \Delta G^{\text{bulk}} + 8\sigma\varphi R^2(2 + \varphi)$;
 $\Delta G(v, x_c) := \min_{\varphi} \Delta G(\varphi, v, x_c)$;
 End of cycle for φ .
 $\Delta G(x_c) := \max_v \Delta G(v, x_c)$;
 End of cycle for v .
 $\Delta G^* := \min_{x_c} \Delta G(x_c)$;
 End of cycle for x_c .

- ¹P. J. Desré and A. R. Yavari, Phys. Rev. Lett. **64**, 1533 (1990).
²A. M. Gusak, Ukr. Fiz. Zh. (Russ. Ed.) **35**, 725 (1990).
³F. Hodaj, A. M. Gusak, and P. J. Desré, Philos. Mag. A **77**, 1471 (1998).
⁴T. Al-Kassab, H. Wollenberger, G. Schmitz, and R. Kirchheim, in *High-Resolution Imaging and Spectrometry of Materials*, edited by F. Ernst and M. Rühle (Springer, Berlin, 2003).
⁵J. Schleiwies and G. Schmitz, Mater. Sci. Eng., A **327**, 94 (2002).
⁶V. Vovk, G. Schmitz, and R. Kirchheim, Phys. Rev. B **69**, 104102 (2004).
⁷E. Emeric, Ph.D. thesis, Marseille University, 1998.
⁸M. O. Pasichnyy, V. Vovk, and A. M. Gusak, in *Proceedings of*

- the 15th International Symposium on Thin-Films in Optics and Electronics, 2003*, edited by A. I. Kuzmichev, V. I. Lapshin, and V. M. Shulayev (Constanta, Kharkiv, 2003), p. 128.
⁹U. Gosele and K. N. Tu, J. Appl. Phys. **53**, 3252 (1982).
¹⁰F. Hodaj and A. M. Gusak, Acta Mater. **52**, 4305 (2004).
¹¹F. M. d'Heurle, P. Gas, J. Philibert, and S. L. Zhang, Defect Diffus. Forum **194–199**, 1631 (2001).
¹²F. Hodaj and P. J. Desré, Acta Mater. **44**, 4485 (1996).
¹³A. M. Gusak, F. Hodaj, and A. O. Bogatyrev, J. Phys.: Condens. Matter **13**, 2767 (2001).
¹⁴P. J. Desré, Acta Metall. Mater. **39**, 2309 (1991).